Three-dimensional bone CT reconstruction anatomy of the vidian canal*

Shao-Cheng Liu[1], Hsing-Won Wang[1], Hao-Lun Kao[2], Po-Chou Hsiao[3], Wan-Fu Su[3]

[1] Department of Otolaryngology-Head and Neck Surgery, Tri-Service General Hospital, National Defense Medical Center, Taipei, Taiwan, Republic of China

[2] Department of Radiology, Tri-Service General Hospital, National Defense Medical Center, Taipei, Taiwan, Republic of China

[3] Department of Otolaryngology-Head and Neck Surgery, Buddist Tzu Chi General Hospital, Taipei Branch, Taipei, Taiwan, Republic of China

Rhinology 51: 0-0, 2013
DOI:10.4193/Rhino12.189

***Received for publication:** November 9, 2012
Accepted: April 25, 2013

Summary

Objectives: To examine the anatomical features of the anterior opening of the vidian canal using three-dimensional (3D) computed tomography (CT) images of the bone.

Methods: We reviewed 62 patients who had undergone bilateral vidian neurectomies. One hundred and twenty-four vidian canals and their surrounding anatomies were analyzed. 3D images were reconstructed using algorithms and compared with conventional two-dimensional (2D) CT images.

Results: A bony prominence that overlaid the vidian canal along the sphenoid sinus floor was found in 60 (48.39 %) canals. Pneumatization of the pterygoid process was observed in 45 sides (36.29%). No significant discrepancy was found in detecting these variances between the 2D and the 3D images. The presence of a surgically favorable gap between the palatine and the sphenoid bone was seen in 25 sides (20.16%) without significant association with pterygoid process pneumatization or vidian canal protrusion. This gap was not identified on the 2D CT scans.

Conclusion: 3D CT reconstruction images of bone provide superior delineation of the gap between the palatine and the sphenoid bone, which is a critical variation for vidian neurectomy. This useful method may contribute to better prediction and guidance of the surgical approach to the vidian canal and pterygopalatine fossa.

Key words: Three dimensional CT sphenoid sinus, vidian canal, vidian neurectomy, pterygoid process

Introduction

Chronic rhinitis is a common pathophysiological process that affects individuals of all ages. The backbone of therapy remains the use of topical and systemic medications. Although surgery is not a primary intervention for treating chronic rhinitis, a vidian neurectomy can be an option because it inhibits excessive efferent stimulation of the parasympathetic system and interrupts cholinergic innervation to the nasal mucosa. However, some otolaryngologists still debate its application in patients with allergic rhinitis. In our opinion, the pathophysiology of the chronic rhinitis commonly overlaps two or more of these classes: allergic, vasomotor, structural and infectious [(1)]. Once treatment for one of these classes, such as the vasomotor component, has started, the threshold for a stimulant to cause symptoms might be elevated, leading to reduced symptoms. Some studies [(2,3)] also show that denervation will lead to a significant reduction of stromal oedema and eosinophilic cellular infiltration, a reduction in mast cell levels and histamine concentrations, and a

reduction of the contents of the acini of mucosal glands, all of which are vital contributors to allergic rhinitis. However, such surgical intervention is not popular owing to the predisposition of anatomical variations to complicate surgery of the skull base. These factors have impeded surgery from gaining acceptance by otolaryngologists.

Recently, we have developed a simple method to undertake a vidian neurectomy. This method is able to spare sphenopalatine artery ligation and can be duplicated by an occasional endoscopist [4,5]. In our surgical experiences of 374 patients, an important anatomical relationship – the synostoses formed by the sphenoid bone and the sphenoid process of the palatine bone – has been noted. The magnitude of vidian nerve obstruction by these synostoses determined the success rate of a precise nerve cut. However, this variation cannot be defined by a review of the previous literature about the structure of the sphenoid sinus, whether based on image analysis [6] or cadaver dissections [7]. Hence, we try to reconstruct three-dimensional (3D) computed tomography (CT) scans to explore the anatomy of this region.

This study aims to examine the anatomical features of the vidian canal when reconstructed using 3D CT images. We focus on the variation of the anterior opening of the vidian canal and its surrounding structure. We also try to show the value of 3D CT reconstruction imaging in this region. The advantages and clinical application will be discussed by comparing the results with traditional (two-dimensional (2D)) CT scans.

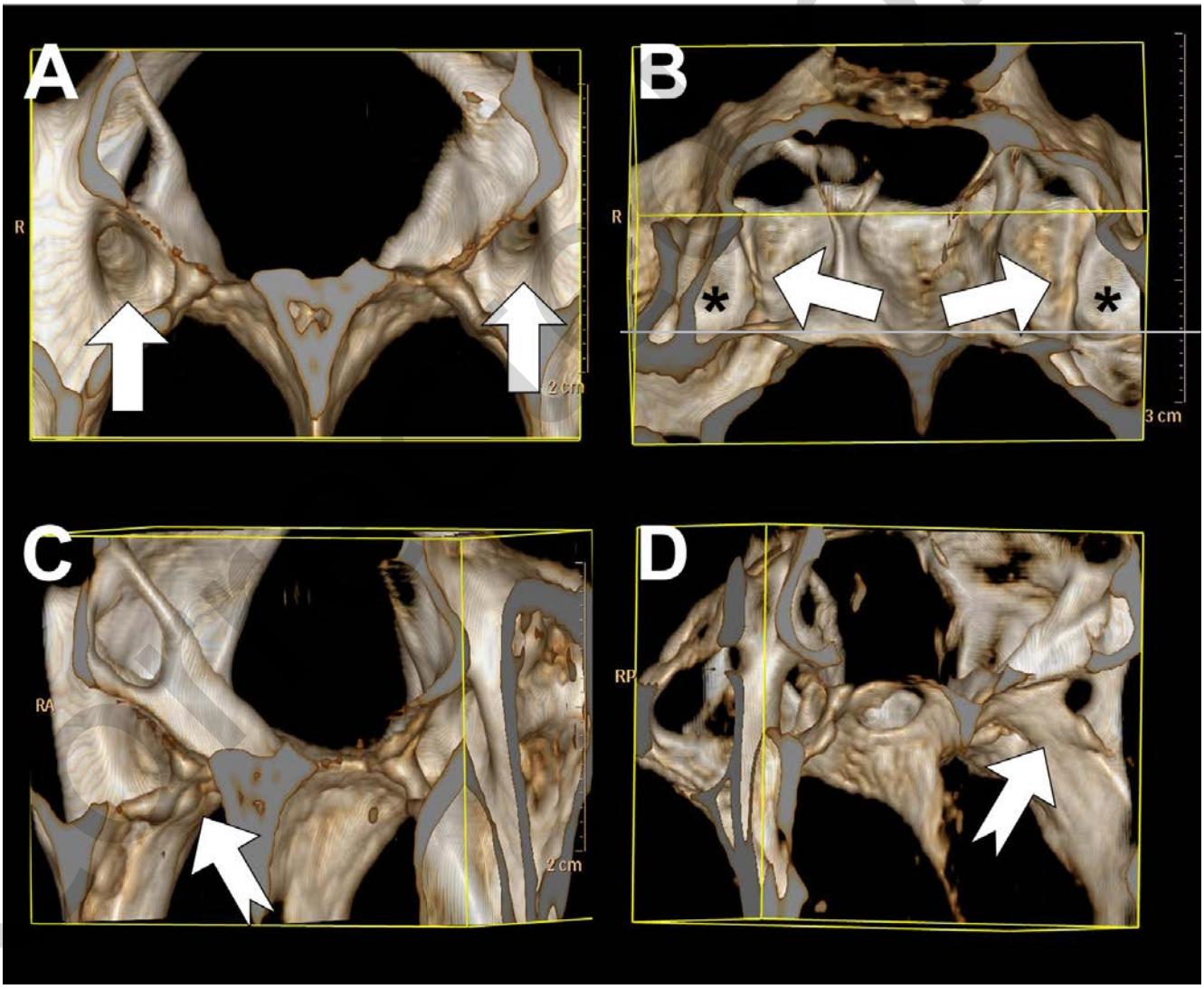

Figure 1. The 3D reconstruction slides of the volume rendering images in different patients. A: on this anteroposterior view, white arrows demonstrate the bilateral anterior opening of vidian canals. B: The caudal rotation view shows the canal protrusion with the presence of lateral pterygoid process pneumatization (black asterisk). C~D: Lateral rotation reveals the contact region (bifid-tail arrow) between the palatine and the sphenoid bone. Pronounced synostoses are observed without surgically available gap formation in this case.

Materials and methods

Procedure

Our surgical techniques have been published in a previous study [8]. There were two approaches to surgery. The type I approach was used if the prominence over the vidian canal in the floor of the sphenoid sinus could be unroofed directly in the sinus cavity without resection of the sphenoid body or pterygoid process. The type II approach was managing the vidian nerve through its anterior opening into the pterygopalatine fossa (PPF) via the additional removal of part of the sphenoid wall and sphenoid process of the palatine (SPP) bone. The accuracy of vidian nerve management was ranked as a precise nerve cut, a semi-precise nerve cut (total resection of vidian canal contents), or cauterization of the vidian canal contents (with an uncertain nerve cut).

Between September 2007 and May 2011, 374 endoscopic vidian neurectomies were performed or supervised by the corresponding author, the senior otolaryngologist consultant (Wan-Fu Su) at the Tri-Service General Hospital and Buddhist Tzu Chi General Hospital, Taipei Branch, Taiwan. Among those cases, a retrospective study of CT images and chart reviews was conducted between June 2009 and May 2011. Sixty-two Taiwanese patients who had undergone bilateral type II endoscopic vidian neurectomies with pre-operative paranasal sinus CT scans were included. All patients were diagnosed as having allergic rhinitis according to their allergy history, serum IgE, a serum allergen test, and a skin prick test. They all showed poor treatment response to a three-month trial of corticosteroid nasal sprays. None had a history of previous nasal or paranasal sinus surgery,

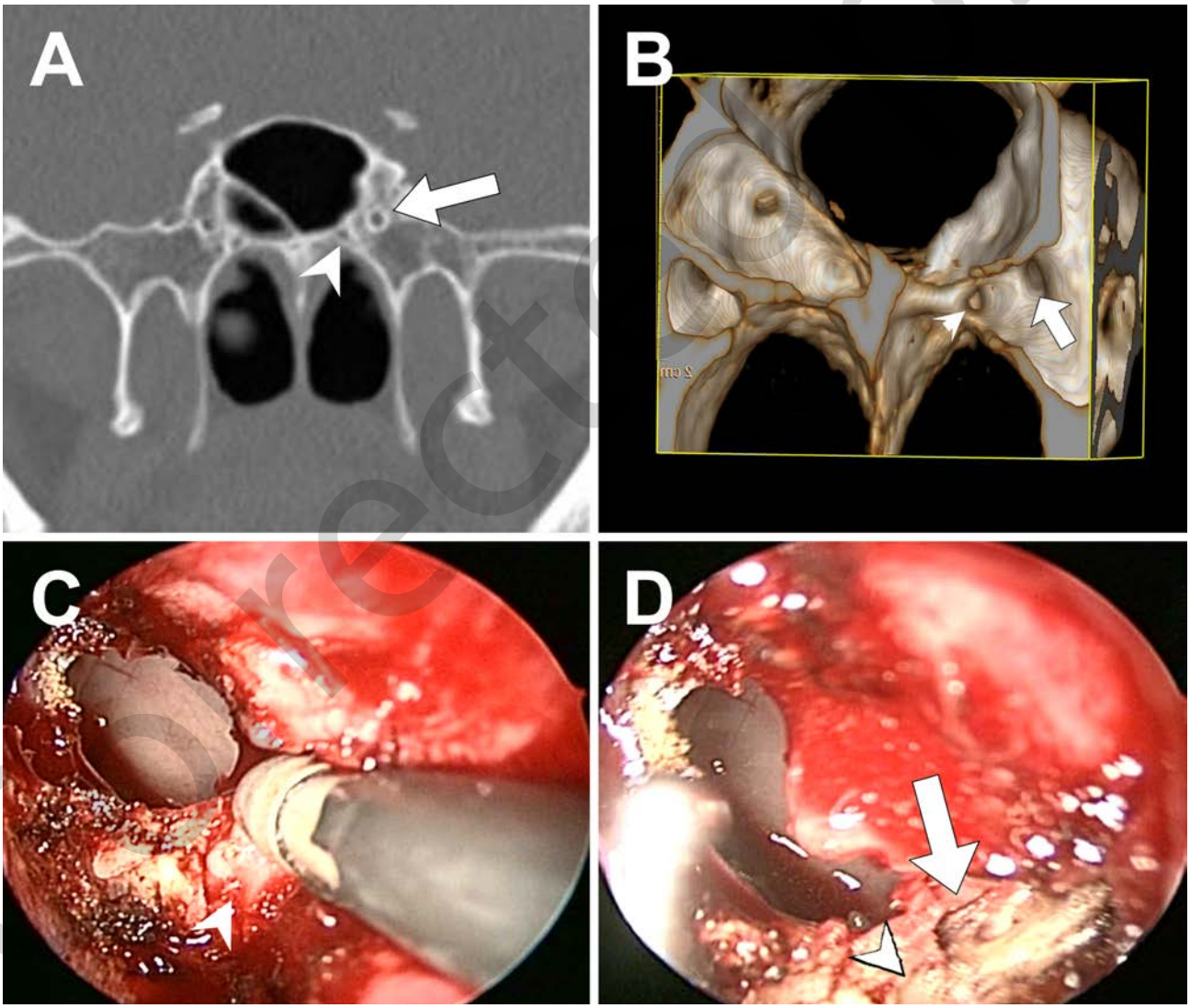

Figure 2. The left side palatovaginal canal (arrow head) located medially to the vidian canal (white arrow) is clearly demonstrated on A: coronal CT slice; and even more realistically in B: 3D reconstruction image. The intraoperative endoscopic view delineates the close relationship of those two nerves (C, D), which may confuse the novice surgeon.

Table 1. Summary of 3D and 2D CT images finding in 124 sides.

Anatomy variances	sides / %		p-value
	3D	2D	
Vidian canal protrusion	60 / 48.39 %	60 / 48.39 %	NS
Pterygoid recess pneumatization	45 / 36.29 %	45 / 36.29 %	NS
Palatovaginal canal	50 / 40.32 %	48 / 38.71 %	NS
Foramen rotundum protrusion	14 / 11.29 %	14 / 11.29 %	NS
Gap visualization	25 / 20.16 %	0 / 0 %	< 0.001

Test applied: Student t test

Table 2. Kappa statistics and 95% confidence intervals (CI) of inter-observer agreement.

Anatomy variances	Kappa	95% CI	Agreement
2D			
Vidian canal protrusion	1.000	(1.000-1.000)	Perfect
Pterygoid recess pneumatization	1.000	(1.000-1.000)	Perfect
Palatovaginal canal	0.941	48 / 38.71 %	Good
Foramen rotundum protrusion	1.000	(1.000-1.000)	Perfect
Gap visualization	1.000	(1.000-1.000)	Perfect
3D			
Vidian canal protrusion	1.000	(1.000-1.000)	Perfect
Pterygoid recess pneumatization	1.000	(1.000-1.000)	Perfect
Palatovaginal canal	1.000	(1.000-1.000)	Perfect
Foramen rotundum protrusion	1.000	(1.000-1.000)	Perfect
Gap visualization	0.938	(0.919-0.953)	Good

tumoral disease, chronic paranasal sinusitis, nasal polyposis, or nasal trauma.

The CT images were obtained using a multiple detector scanner (Philips Brilliance 64 slice CT scanner, Philips Medical Imaging, Best, the Netherlands). The imaging parameters were 120 kVp; 150 mAs; gantry rotation time 0.5 s; beam width 0.625 mm; beam pitch 0.64; and table speed 51.2 mm/s. The scanning area extended from the frontal sinus roof to the superior alveolar ridge. CT images were directed in the coronal, sagittal, and axial planes using an algorithm with 1 mm contiguous sections. The axial images were obtained parallel to the plane between the hard palate and the foramen magnum, while the coronal images were reformatted perpendicularly to the hard palate. The sagittal image was perpendicular to the coronal image. A 3D projected view directly from the volume data (volume rendering) was created (window width, 2500; window level, 200). Three views of 3D images of the bone were reconstructed as follows: the anteroposterior, the 45 degree caudal rotation, and the 45 degree lateral rotation views (Figure 1).

We focused on four specific anatomical areas. First, the sphenoid sinus was analyzed throughout its length. The pneumatization pattern of the sphenoid bone, including the pterygoid process, was assessed. Pterygoid process pneumatization (pterygoid recess, PR) was defined when sinus pneumatization extended beyond a horizontal plane crossing the vidian canal. Second, the anterior opening of the vidian canal was addressed. Before the vidian nerve joined the pterygopalatine ganglion in the PPF, synostoses of the sphenoid bone and the SPP usually bounded its medial side. From the surgical experiences of 374 patients, the magnitude of vidian nerve obstruction by these synostoses determined the success rate of a precise nerve cut [8]. Third, the position of the vidian canal relative to the sphenoid bone was determined. The relationship between the canal and the sphenoid bone (canal corpus type) [5] can be categorized according to the presence of a bony prominence that overlaid the vidian canal along the sphenoid sinus floor. Three groups were defined: 1) embedded inside the sphenoid corpus, 2) partially protruding, and 3) connected to the bone with a stalk inside the sinus. A completely embedded vidian canal gave no surgical guide in nerve identification. Fourth, the foramen rotundum on the lateral side and the palatovaginal canal on the medial side were identified to prevent them from being mistaken as the vidian canal (Figure 2).

Statistical analysis

In addition to 3D reconstruction images of bone, the abovementioned anatomic variations were read carefully from the coronal and axial CT slices with 1 mm contiguous sections. Four authors (SCL, HWW, HLK, WFS) reviewed detailed analyses of both 2D

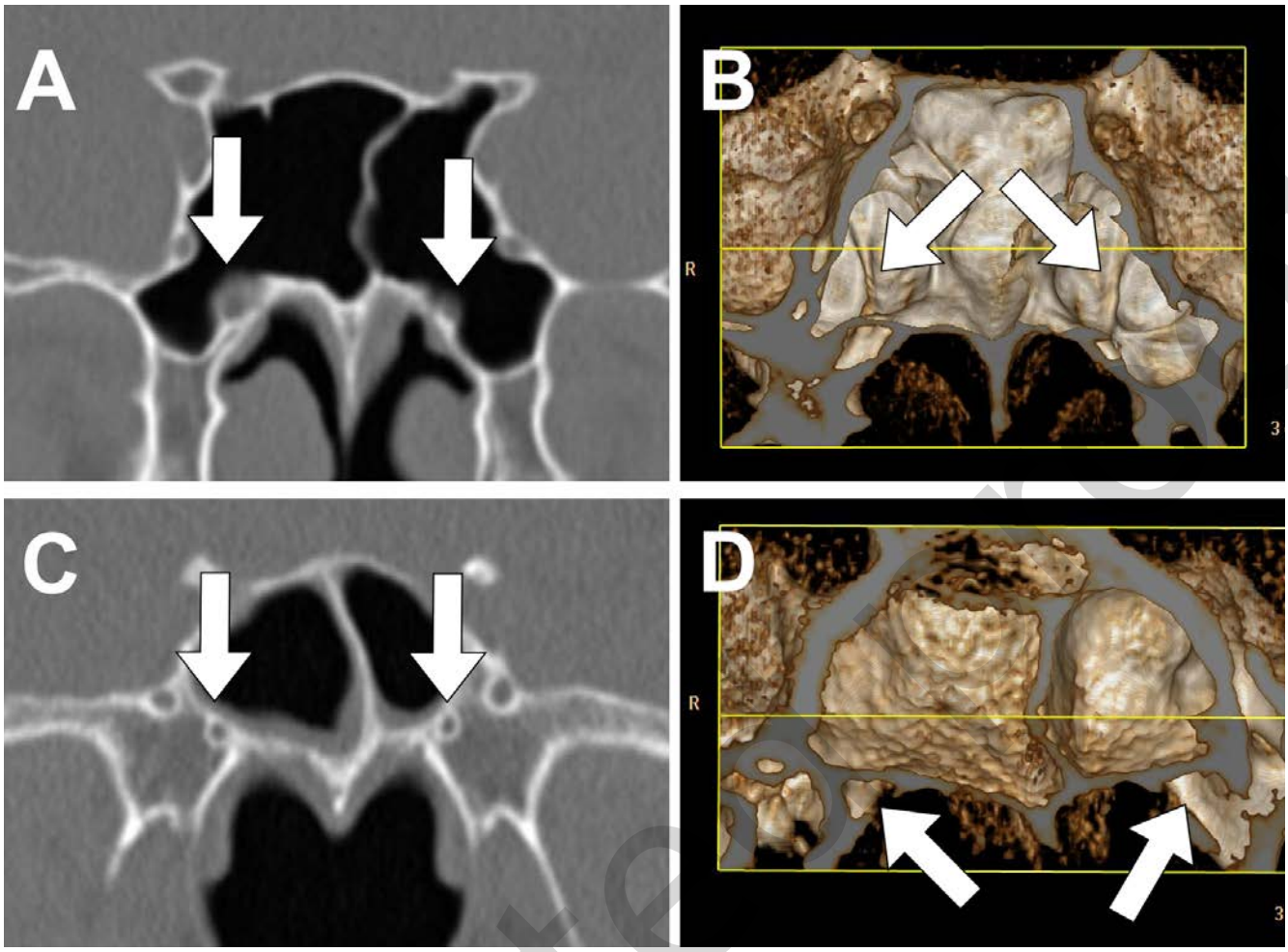

Figure 3. Different canal-corpus relationships according to the presence of a bony prominence that overlaid the vidian canal (white arrow) along the sphenoid sinus floor: A~B: A coronal CT slice and 3D image shows the bony prominence of the vidian canal. C~D: A completely embedded vidian canal is shown and the infeasibility of intra-sphenoid vidian neurectomy can be predicted by the 3D image.

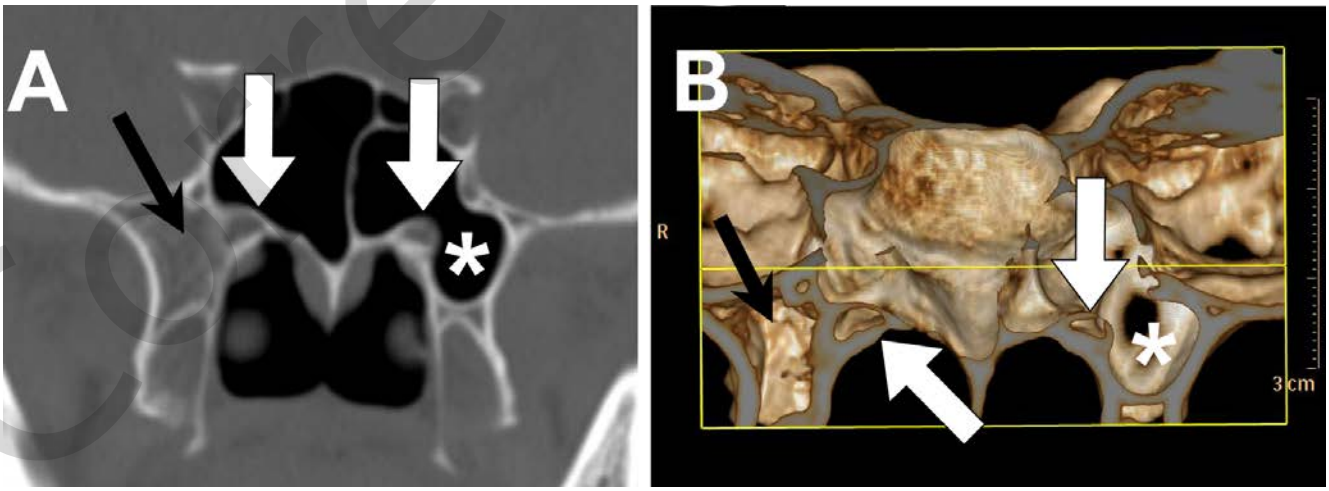

Figure 4. The coronal CT slice (A) and 3D reconstruction image (B) delineate the variation of pterygoid process pneumatization (pterygoid recess, PR). The PR is present on the left side (asterisk) but absent on the right side (black arrow). Bilateral vidian canal protrusion (white arrow) is also demonstrated.

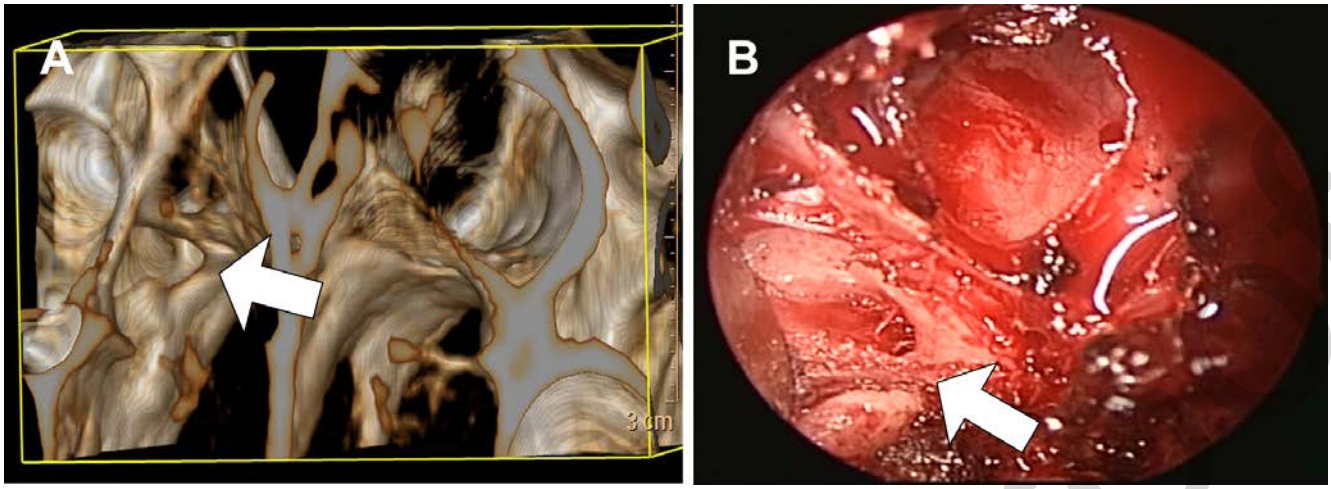

Figure 5. The gap (white arrow) between the sphenoid bone and sphenoid process of the palatine bone is shown on A: a pre-operative 3D reconstruction CT image; and B: an intraoperative endoscopic view.

and 3D CT scans, including the frequency of each of the four described anatomical features, and the discrepancies between the results obtained by 2D and 3D images were recorded. Both the chi-squared test and Student's t test were used for statistical analysis; differences were assumed significant at $p < 0.05$. Meanwhile, the interobserver agreement was assessed by calculating kappa (κ) statistics.

Ethical considerations

The Buddhist Tzu Chi General Hospital Taipei Branch Institutional Review Board reviewed and approved the research protocol. Each eligible subject gave his or her informed consent before enrolment into the study.

Results

Sixty-two cases were analyzed in this study: 26 men and 36 women, with a mean age of 31 (between 20 and 65 years) years. All 124 vidian canals were imaged successfully and each side was evaluated separately. Table 1 shows the summary of the findings from both the 3D and 2D images. The canal was embedded inside the sphenoid corpus in 64 sides (51.61%) and a bony prominence overlaid the vidian canal along the sphenoid sinus floor in 60 (48.39 %) canals (Figure 3). Pneumatization of the pterygoid process was noticed in 45 sides (36.29%) (Figure 4). No discrepancy in detecting these variances was observed between the 2D and 3D CT reconstruction images. Coexistence of PR and vidian canal protrusion was found in 34.68% (43/124) of the cases. Statistically, there was significant association between PR and vidian canal protrusion ($p < 0.05$). Table 2 showed the κ-scores for interobserver agreement among examiners. The overall interobserver agreement for all observers was almost perfect for all variables. We also found that the 3D images have better interobserver agreement than the 2D images in identifying the presence of the palatovaginal canal.

Table 3. Correlation of gap visualization with anatomical variations of surrounding structure.

	Gap visualization		p-value
	+	-	
Pterygoid recess pneumatization	13	31	0.068
Vidian canal protrusion	13	47	0.686

Test applied: Chi-square

On the medial side, the palatovaginal canal could be recognized in 50 sides (40.32%) by 3D reconstruction images of the bone. On the lateral side, the foramen rotundum showed protrusion in 14 sides (11.29%). The palatovaginal canal was overlooked in two cases by analyzing 2D coronal CT, but foramen rotundum protrusion can be identified without negligence.

The presence of a gap between the SPP and sphenoid bone was seen in 25 sides (20.16%) from the 3D reconstruction images. The remaining 99 sides presented pronounced synostoses between the palatine and the sphenoid bone (Figure1, C~D). No such information could be identified from traditional 2D CT scans. This favorable anatomical variance with a gap significantly facilitated the nerve severance during our surgical approach (Figure 5). Statistical analysis revealed no relationship between the gap prevalence and the presence of PR ($\chi^2 = 3.342$, $p = 0.068$) or vidian canal protrusion ($\chi^2 = 0.164$, $p = 0.686$) (Table 3).

Discussion

In fetal life, the sphenoid bone consists of two main parts: the pre-sphenoid and post-sphenoid parts. The pre-sphenoid part lies in front of the tuberculum and is continuous with the small wings. The post-sphenoid part comprises the sella turcica and dorsum sellae, which are associated with the great sphenoid wings and pterygoid processes [9]. The bone is ossified from cartilage. There are 14 centers in all, 6 for the pre-sphenoid part and 8 for the post-sphenoid part, which appear in about the eighth to ninth week of fetal life. Before joining, both medial and lateral pterygoid plates are ossified in membrane and their centers probably appear at about the ninth or tenth week of fetal life. The pre-sphenoid part is united with the post-sphenoid part at about the eighth month of fetal life, and the great wings and body are united in the first year after birth. Those fused lines are hardly recognizable in adults. The remains of the craniopharyngeal canal are occasionally visible between the pre- and post-sphenoid bones, through which the hypophyseal diverticulum of the buccal ectoderm is transmitted in early fetal life [10]. The sphenoid sinuses are present as minute cavities at the time of birth, but do not attain their full size until after puberty.

The vidian canal, also called the pterygoid canal, is located in the line of fusion between the pterygoid process and the sphenoid body [11]. It conveys the vidian nerve, which is formed by the union of the greater superficial and deep petrosal nerves in the carotid canal. The vidian nerve exits the lateral part of the anterior end of the carotid canal, passes along the upper part of the anterolateral edge of the foramen lacerum, courses through the vidian canal, and ends in the pterygopalatine ganglion in the posterior part of the PPF [6]. In its anterior opening leaving the sphenoid sinus, the vidian nerve is positioned on the superomedial part of the anterior surface of the pterygoid process, at the level of the floor of the sphenoid sinus, inferomedial to the foramen rotundum and lateral to the upper part of the nasopharynx [12]. The pterygoid process forms the posterior wall of the PPF, while the perpendicular plate of the palatine bone forms its medial wall [13,14]. The upper part of the perpendicular plate is the site of the sphenopalatine notch, a U-shaped opening. The anterior margin of the notch is formed by the orbital process, which extends upward to form a small portion of the posterior part of the floor of the orbit. The posterior margin of the notch is formed by the sphenoid process, which articulates with the sphenoid bone just medial to the vidian canal [7]. In adults, the contact between the palatine bone and the surrounding bones is usually pronounced, and the bony bridge formation across the suture is characterized by many synostoses. If the join between the SPP and the sphenoid bone is loose or low enough to allow the passing through of the probe into the vidian canal opening, the type II surgical approach will have a significantly higher success rate of precise nerve severance [5]. Some patients even show a prominent gap, and the vidian canal is covered only by soft tissue. Otherwise, if the join is too high or tight to allow this procedure, the pterygoid process or SPP needs to be partially removed and the accuracy of vidian nerve management may fall into a semi-precise nerve cut or cauterization of the vidian canal contents [8]. Sometimes, the canal opening is not easily accessible due to obscuration by the pronounced synostoses. A 3D image may offer better prediction and guidance for surgery.

The development of paranasal sinuses begins prenatally and continues throughout life. Between 1 and 7 years of age, paranasal sinuses continue their expansion in all directions as development of the nasal cavity and other facial structures expand. It is nearly complete between 12 and 14 years of age and by then has reached adult proportions [15]. The degree of development of paranasal sinuses differs from person to person and from side to side in the same individual. The sphenoid sinus and its adjacent bony structures may show various degrees of pneumatization. Initial signs of pneumatization for the sphenoid sinus are observed at 9 months. The sphenoid sinus develops quickly after the age of 3 years and spreads back toward the sella turcica around the age of 7 years, reaching adult form at around the age of 12 to 15 years. The anterior clinoid and pterygoid processes are frequent sites of variable pneumatization in the skull base, leading to the protrusion of an underlying neurovascular bundle: the optic canal and vidian canal. On occasion, pneumatization can be so extensive that it can even surround the maxilloethmoid recess [16]. Protrusion of the vidian canal will give a good surgical guide in endoscopic vidian neurectomy, which can be performed inside the sphenoid (type I) or over its anterior opening of the sphenoid bone (type II) [5]. In patients with a vidian canal that is completely embedded, nerve identification is only enabled by its relation to the pterygoid process, the SPP, and even the floor or lateral wall of the sphenoid sinus. In this situation, 3D imaging provides better and more detailed spatial information than a 2D image does.

Kazkayasi et al. reviewed paranasal sinus CT scans of 267 patients (534 sides) and stated that vidian canal protrusion was found in 158 sides (29.6%), with pterygoid process pneumatization found in 164 sides (30.7%). There was a statistically significant correlation between these two structures [17]. Our analysis obtained a similar result, showing a coexistence of PR and vidian canal protrusion in 34.68% (43/124) of cases with statistical significance. This was expected since the vidian canal lies in the fusion line between the pterygoid process and the sphenoid body. However, neither the degree of pterygoid process pneumatization nor vidian canal protrusion was found to be significantly related to the presence of a favorable gap formed by the palatine and the sphenoid bone. No cases with palatine bone pneumatization can be found in the literature and the relationship between degree of sphenoid sinus pneumatization and palatine bone development is poorly understood. Melsen et al. once performed a macroscopic and microscopic study of dry skulls from age 0 to 27 [18]. In the infantile stage, the palatine

bone was clearly separated from the pterygoid process by wide, slightly irregular layers of connective tissue, leaving the palatine bone freely movable between the maxilla and the sphenoid bone. The SPP and the sphenoid bone were seen to approach each other through a sheet of loose fibrous tissue. Histological examination showed both osteoblast and osteoclast cells covering 60% to 70% of the bone surfaces, suggesting that modeling leading to a change in morphology was in progress. In the juvenile stage, the connection between the palatine bone and the pterygoid process was smooth and only minor remodeling seemed to have taken place. In the adolescent stage, there was increased contact surface between the pterygoid process and palatine bone, indicating a high level of remodeling activity. At the same time, pneumatization of the sphenoid sinus continued. Therefore, the degree of sphenoid sinus pneumatization, especially the pterygoid process, should effect synostoses formation between the palatine and the sphenoid bone. However, according to our analysis, the presence of a surgically favorable gap between the palatine and the sphenoid bone was not correlated with pneumatization of the pterygoid process or vidian canal protrusion.

Although direct CT scanning at 1 mm sections is often adequate for the evaluation of most sinonasal and skull base structures, it has some limitations. Based on our report, the gap between the palatine and the sphenoid bone cannot be traced from traditional fine-cut CT images and cannot be predicted from its surrounding anatomical features. It can only be illustrated by 3D CT reconstruction images of the bone. The presence of this gap is critical in the type II approach to surgery. Therefore, a distinct value of 3D CT scanning is evident, and we suggest three standard views for interpretation: the anteroposterior, the 45 degree caudal rotation, and the 45 degree lateral rotation views. The vidian canal protrusion, its relation with the sphenoid corpus, the pterygoid process pneumatization, and most importantly, the gap between the palatine and the sphenoid bone can be delineated thoroughly in these three views. Finally, palatovaginal canals are easily depicted on 3D images. This canal is a short bone tunnel that extends from the PPF to the roof of the pharynx. It is formed by the application of the SPP to the vaginal process of the sphenoid bone. The palatovaginal canal is found inferomedially on the posterior wall of the PPF [19]. The canal transmits the pterygovaginal artery (pharyngeal artery and descending pharyngeal artery), a posterior branch of the internal maxillary artery, and the pharyngeal nerve from the pterygopalatine ganglion to the pharyngeal orifice of the auditory tube. Owing to its small size, when using 1 mm 2D coronal slices, the palatovaginal canal was overlooked in two cases in this study, compared with images reconstructed from the 3D scans. In our surgical experience, this canal sometimes confuses novice surgeons and the preoperative 3D CT images would be helpful in this situation.

In our country, no further cost is incurred in performing 1 mm cut paranasal sinus CT compared with 3 mm cut sinus CT, and the reconstruction for those four views takes radiological technicians about 2 minutes to collect. Hence, 3D CT imaging is both low-cost and efficient. Therefore, we suggest it be considered as a supplementary examination tool if the pterygopalatine area or the vidian canal need to be addressed.

Conclusion

In conclusion, understanding the regional anatomy of and around the vidian canal may decrease the possibility of surgical complications associated with an endoscopic vidian neurectomy. In comparison with 2D CT images, 3D CT images provide an extra benefit in delineating the anatomy of the related area.

Acknowledgement

The project was partly supported by TSGH-C100-138.

Authorship contribution

SCL: data collection, writer, literature search, images review, article submission; HWW: article and images review; HLK: images review; PCH: article review; WFS: study design, images review, review/editing.

Conflict of interest

None.

References

1. International Consensus Report on the diagnosis and management of rhinitis. International Rhinitis Management Working Group. Allergy. 1994; 49: 1-34.
2. Mostafa HM, Abdel-Latif SM, el-Din SB. The transpalatal approach for Vidian neurectomy in allergic rhinitis. J Laryngol Otol. 1973; 87: 773-780.
3. Kamel R, Zaher S. Endoscopic transnasal vidian neurectomy. Laryngoscope. 1991; 101: 316-319.
4. Liu SC, Su WF. Evaluation of the feasibility of the vidian neurectomy using computed tomography. Eur Arch Otorhinolaryngol. 2011; 268: 995-998.
5. Liu SC, Wang HW, Su WF. Endoscopic vidian neurectomy: the value of preoperative computed tomographic guidance. Arch Otolaryngol Head Neck Surg. 2010; 136: 595-602.
6. Yazar F, Cankal F, Haholu A, Kilic C, Tekdemir I. CT evaluation of the vidian canal localization. Clin Anat. 2007; 20: 751-754.
7. Osawa S, Rhoton AL, Jr., Seker A, Shimizu S, Fujii K, Kassam AB. Microsurgical and endoscopic anatomy of the vidian canal. Neurosurgery. 2009; 64: 385-411.
8. Su WF, Liu SC, Chiu FS, Lee CH. Antegrade transsphenoidal vidian neurectomy: Short-term surgical outcome analysis. Am J Rhinol Allergy. 2011; 25: 217-220.
9. Catala M. [Embryology of the sphenoid bone]. J Neuroradiol. 2003; 30: 196-200.
10. Ekinci G, Kilic T, Baltacioglu F., et al. Transsphenoidal (large craniopharyngeal) canal associated with a normally functioning pituitary gland and nasopharyngeal extension, hyperprolactinemia, and hypothalamic hamartoma. AJR Am J Roentgenol. 2003; 180: 76-77.
11. Omami G, Hewaidi G, Mathew R. The

neglected anatomical and clinical aspects of pterygoid canal: CT scan study. Surg Radiol Anat. 2011; 33: 697-702.
12. Vescan AD, Snyderman CH, Carrau RL., et al. Vidian canal: analysis and relationship to the internal carotid artery. Laryngoscope. 2007; 117: 1338-1342.
13. Fortes FS, Sennes LU, Carrau RL., et al. Endoscopic anatomy of the pterygopalatine fossa and the transpterygoid approach: development of a surgical instruction model. Laryngoscope. 2008; 118: 44-49.
14. Isaacs SJ, Goyal P. Endoscopic anatomy of the pterygopalatine fossa. Am J Rhinol. 2007; 21: 644-647.
15. Adibelli ZH, Songu M, Adibelli H. Paranasal sinus development in children: A magnetic resonance imaging analysis. Am J Rhinol Allergy. 2011; 25: 30-35.
16. Lu Y, Pan J, Qi S, Shi J, Zhang X, Wu K. Pneumatization of the sphenoid sinus in Chinese: the differences from Caucasian and its application in the extended transsphenoidal approach. J Anat. 2011; 219: 132-142.
17. Kazkayasi M, Karadeniz Y, Arikan OK. Anatomic variations of the sphenoid sinus on computed tomography. Rhinology. 2005; 43: 109-114.
18. Melsen B, Ousterhout DK. Anatomy and development of the pterygopalatomaxillary region, studied in relation to Le Fort osteotomies. Ann Plast Surg. 1987; 19: 16-28.
19. Rumboldt Z, Castillo M, Smith JK. The palatovaginal canal: can it be identified on routine CT and MR imaging? AJR Am J Roentgenol. 2002; 179: 267-272.

Wan-Fu Su, M.D.
Associate Professor
Department of Otolaryngology-Head and Neck Surgery
Buddist Tzu Chi General Hospital Taipei Branch
No.289, Jianguo Rd., Xindian Dist.
New Taipei City 23142
Taiwan, R.O.C

Tel: +886-2-8792-7192
Fax: +886-2-8792-7193
E-mail: wfs19582001@yahoo.com.tw